Quarks and Nucleons: A General Relativistic Perspective on Strong Forces

Y. Sobouti,[1,*] S. Nasiri,[1,†] M. Bigdeli,[2,‡] S. Aslani,[1,§] S. Bazargan,[1,¶] and E. Bakhshi[1,**]

[1] *Department of Physics, Institute For Advanced Studies in Basic Sciences (IASBS), Zanjan 45137-66731, Iran*

[2] *Department of Physics, University of Zanjan, P.O. Box 45371-38791, Zanjan, Iran*

(Dated: July 19, 2026)

Quarks, as massive entities, are capable of curving their surrounding spacetime and, as spin-1/2 particles, can be considered as *normalizable* Dirac spinors. In this paper, we demonstrate that the general relativistic (GR) gravitation of quarks is sufficient to confine them within hadrons while simultaneously allowing them to remain asymptotically free. We conclude that at the femtometer scale of quarks and hadrons, the strong and gravitational forces are one and the same.

I. INTRODUCTION

To the best of our knowledge, two major gaps persist in hadronic physics:

1 There is no established wave function for hadrons or their constituent quarks that parallels, for instance, Dirac waves for electrons.

2 There is no definitive understanding of the exact nature of strong forces, except for the fact that they are strong and confining.

In this paper, we assume that quarks, being massive entities, are capable of curving their surrounding spacetime. Furthermore, as spin-1/2 particles, they can be treated as Dirac spinors provided they are properly normalized. We formulate the Dirac equation in a spherically symmetric and static spacetime, impose a Yukawa-like normalization, and solve the system. Ultimately, we demonstrate that GR forces at femtometer scales are strong enough to confine quarks within nucleons, while allowing them to exhibit asymptotic freedom in the interior regions.

The Dirac equation in curved spacetime has a rich and well-documented history. Attempts to address this problem range from the pioneering works of the founders of quantum mechanics—such as Fock [1], Fock and Ivanenko [2], Nieh and Yan [3], Bargmann [4], Schrodinger [5] to the contributions of late 19^{th} Century writers, Ruffini and Bonazzola [6], Ferrari and Ruffini [7] and to the contemporary works of Brito Cardoso Herdeiro, Radu [8] Herdiero, Pombo, Radu [9], Daka Phan Kain [10], among many others.

The standard Dirac matrices γ^μ are invariant under Lorentz transformations in Cartesian coordinates, but this invariance does not hold in curved ones. In his comprehensive paper [11], Alcubierre transforms the γ matrices into a spherically symmetric spacetime using tetrad analysis. By writing down the Dirac equation, he derives four coupled, first-order differential equations: two for the Dirac field and two for the spacetime metric coefficients. A Yukawa-normalizable version of Alcubierre's four coupled equations serves as our starting point.

The remainder of this paper is organized as follows: In Section II, we provide a formal definition of the problem and outline an iteration scheme for its analysis. In Section III, we explain how a spin-1/2 quark can be modeled as an Alcubierre-designed and Yukawa-normalized Dirac spinor, subsequently constructing the wave function for nucleons. In Section IV, we study the gravitational manifestations of these quarks and nucleons. The spacetime inside and outside the nucleon is non-singular and has a stable point of equilibrium. The asymptotically flat environment of this equilibrium point guarantees the asymptotic freedom of the constituent quarks, while the exponential falloff of the outer spacetime to a flat one ensures their confinement.

II. DEFINITION OF THE PROBLEM

Miguel Alcubierre [11] begins with a spherically symmetric spacetime:

$$ds^2 = -\alpha^2(r)dt^2 + a^2(r)dr^2 + r^2\left(d\theta^2 + \sin^2\theta\, d\phi^2\right) \quad (1)$$

and formulates the corresponding Dirac equation. For positive energy and spin $\pm\frac{1}{2}$, we extract the following spinor representations from his work:

$$\Psi_+(\mathbf{r}) = \frac{1}{\sqrt{2\pi}} e^{+i\phi/2} \begin{bmatrix} f\sin\theta/2 \\ if\cos\theta/2 \\ ig\sin\theta/2 \\ g\cos\theta/2 \end{bmatrix}, \quad (2)$$

$$\Psi_-(\mathbf{r}) = \frac{1}{\sqrt{2\pi}} e^{-i\phi/2} \begin{bmatrix} f\cos\theta/2 \\ -if\sin\theta/2 \\ ig\cos\theta/2 \\ -g\cos\theta/2 \end{bmatrix}. \quad (3)$$

where $f(r)$ and $g(r)$ are two radial functions. In this representation, the spin operator is given by $-i\partial_\phi$, and one can immediately verify that its eigenvalue is $\pm 1/2$,

$$-i\partial_\phi\psi_\pm = \pm\frac{1}{2}\psi_\pm.$$

* sobouti@iasbs.ac.ir
† nasiri@iasbs.ac.ir
‡ m˙bigdeli@znu.ac.ir
§ s.aslani@iasbs.ac.ir
¶ s.bazargan@iasbs.ac.ir
** elnazbakhshi@iasbs.ac.ir

The coupled differential equations governing f, g, α, and a are given by [11]:

$$f' = -f\left(\frac{\alpha'}{2\alpha} + \frac{1}{r}(1-a)\right) - ag\left(\frac{\omega}{\alpha} + m\right), \qquad (4)$$

$$g' = -g\left(\frac{\alpha'}{2\alpha} + \frac{1}{r}(1+a)\right) + af\left(\frac{\omega}{\alpha} - m\right), \qquad (5)$$

$$\alpha' = \alpha\left(\frac{a^2-1}{2r} + 4\pi r a^2 S^r_r\right), \qquad (6)$$

$$a' = a\left(\frac{1-a^2}{2r} + 4\pi r a^2 S^t_t\right). \qquad (7)$$

where the prime ($'$) denotes the derivative with respect to r, while m and ω represent the rest mass and eigenfrequency of the spinor (the quark), respectively. The components of the stress-energy tensor for each spinor are defined as:

$$S^t_t = -\rho_E = -\frac{\omega}{2\pi}(f^2+g^2), \qquad (8)$$

$$S^r_r = \frac{1}{2\pi a}\left(fg' - f'g\right), \qquad (9)$$

$$S^\theta_\theta = S^\varphi_\varphi = \frac{1}{2\pi}\frac{fg}{r}. \qquad (10)$$

Equations (4)–(10) are nonlinear and mutually coupled. However, they can be solved using an iterative approximation scheme.

A. Iteration scheme

To initiate the process, let us assume a baseline flat spacetime where $\alpha = a = 1$. The equations for f, g, α, and a reduce to:

$$f' = -(\omega+m)g, \qquad g' = -\frac{2}{r}g + (\omega-m)f, \qquad (11)$$

$$\alpha' = 4\pi r S^r_r = 2r(fg' - f'g), \qquad (12)$$

$$a' = 4\pi r S^t_t = -2\omega r(f^2+g^2). \qquad (13)$$

From (11) we obtain the following second-order differential equation:

$$r^2 g'' + 2rg' + \left(k^2r^2 - 2\right)g = 0, \quad k^2 = (\omega^2 - m^2), \qquad (14)$$

where k has the dimension of $length^{-1}$ in Planck units ($G = \hbar = c = 1$). Restoring physical units, this relation should be expressed as:

$$k^2 = \left(\frac{\omega^2}{c^2} - \frac{m^2c^2}{\hbar^2}\right) \quad \Rightarrow \quad \hbar^2\omega^2 = \hbar^2k^2c^2 + m^2c^4. \qquad (15)$$

Interpreting $\hbar\omega$ as the total energy of the particle and $\hbar k$ as its momentum, (15) is readily recognized as the relativistic energy-momentum relation for the spinor. However, the quantum nature of this relation imposes a constraint. If $\Delta r \approx r_{nuc}$ represents the physical size of a nucleon and $\Delta p \approx \hbar k_{min}$ is its minimum momentum, Heisenberg's uncertainty principle demands that:

$$\begin{aligned} &\Delta p\Delta r \approx \hbar k_{min}\, r_{nuc} \approx \hbar \qquad \text{or} \\ &k^{-1}_{min} \approx r_{nuc} \quad \text{of order femtometer.} \end{aligned} \qquad (16)$$

Further order-of-magnitude estimates yield:

$$\hbar\omega_{min} \approx \hbar k_{min} c \approx 197, \qquad (17)$$

The estimation of k_{min}, (16), is rooted in the uncertainty principle, which fundamentally requires the spinor wavelength to fit inside the nucleon boundary. This constraint requires that $\hbar k_{min} c$ must be roughly 50 to 60 times larger than the rest energy of the quarks(17). As will be discussed in Section IV C, this same property explains why nucleon masses are approximately 100 times larger than the combined rest masses of their constituent quarks.

B. Yukawa amelioration

Equation (14) is a spherical Bessel equation of order $n = 1$. Its standard solutions (spherical Bessel functions of the first and second kind) are not square-normalizable over all space. To tame divergences, a Yukawa-like amelioration is required. This is achieved by allowing the wave vector k to acquire an imaginary component (see [12] for an analogous Yukawa-like regularizing treatment of Klein-Gordon waves). To implement this provision, we introduce the following complex variables:

$$K_\pm = k \pm i\kappa, \quad K^2 = K_+K_- = (k^2+\kappa^2),$$

$$z = \frac{K_+}{K}r, \quad \frac{\partial}{\partial z} = \frac{K_-}{K}\frac{\partial}{\partial r}, \quad r = \frac{K_-}{K}z, \quad \frac{\partial}{\partial r} = \frac{K_+}{K}\frac{\partial}{\partial z},$$

where κ has dimensions of $length^{-1}$ and, like k must be on the order of fm^{-1}. Consequently, (14) takes the form:

$$z^2\partial_z^2 g + 2z\partial_z g + (K^2z^2 - 2)g = 0. \qquad (18)$$

For the complexified f of (11) and g of (18), we find two independent sets of solutions:

$$f_i = \frac{\sin Kz}{Kz} = \left(1 - \frac{1}{6}K^2z^2 + \cdots\right), \qquad (19)$$

$$\begin{aligned} g_i &= -\frac{K_-}{K}\left(\frac{\cos Kz}{Kz} - \frac{\sin Kz}{K^2z^2}\right) \\ &= -\frac{K_-}{3K}Kz\left(1 - \frac{1}{10}k^2z^2 + \cdots\right), \end{aligned} \qquad (20)$$

$$f_e = \frac{e^{iKz}}{Kz}, \qquad (21)$$

$$g_e = -\frac{K_-}{K}e^{iKz}\left(\frac{i}{Kz} - \frac{1}{K^2z^2}\right). \qquad (22)$$

Accordingly, the complexified version of the metric coefficients of (12) and (13) for each quark becomes:

$$\alpha' = Kr\big[(f^*g' + fg'^*) - (f'^*g + f'g^*)\big], \tag{23}$$
$$a' = -2\omega Kr(f^*f + g^*g). \tag{24}$$

In the Appendix, we expand $(f_i,\ g_i)$ and $(f_e,\ g_e)$ in terms of standard trigonometric and hyperbolic functions. Their asymptotic behaviors are as follows:

f_i and $g_i \to$ finite as $r \to 0$, and $\to \infty$ as $r \to \infty$.
f_e and $g_e \to \infty$, as $r \to 0$, and $\to 0$ as $r \to \infty$.

Therefore, to construct a physically acceptable, normalizable wave function, we must use the interior solutions (f_i, g_i) up to a specific transition radius r_t, and then match them to the exterior solutions (f_e, g_e) for the outer region. This transition distance should typically be of the order of a fraction of the nucleon radius.

The probability density, which is proportional to $(f^*f + g^*g)$, must remain continuous at r_t. This requires the introduction of a matching parameter, D, to ensure that:

$$(f_i^*f_i + g_i^*g_i)_{r_t} = D^2(f_e^*f_e + g_e^*g_e)_{r_t}. \tag{25}$$

Furthermore, as will be demonstrated later, maintaining continuous derivatives for the metric coefficients α and a at r_t requires the slope of the rising interior branch to be equal to the slope of the falling exterior branch at the transition point. The latter condition is expressed as:

$$(f_i^*f_i' + g_i^*g_i')_{r_t} + c.c. = -D^2\big((f_e^*f_e' + g_e^*g_e')_{r_t} + c.c.\big). \tag{26}$$

Simultaneously solving (25) and (26) uniquely determines both the matching constant D and the transition radius r_t for any given values of k and κ. The global normalization constant N^2 is then defined as:

$$N^2 = \int_0^{r_t} (f_i^*f_i + g_i^*g_i)\, r^2 dr + D^2\int_{r_t}^{\infty} (f_e^*f_e + g_e^*g_e)\, r^2 dr. \tag{27}$$

Detailed expansions of (25), (26), and (27) in terms of real-valued trigonometric and hyperbolic functions are provided in (A11) - (A14) of the Appendix.

Figure 1 illustrates the integrand $(f^*f + g^*g)r^2$, which represents the radial probability density of the spinor. At the transition radius the slopes of its ascending and descending branches are equal. The exterior tail decays exponentially to zero as $e^{-2\kappa r}$.

III. WAVE FUNCTIONS FOR QUARKS AND NUCLEONS

With the foundational mathematical framework established, we now turn to the core thesis of this paper. We propose that the spinors $\Psi_\pm$ given in (2) and (3), with f and g defined by (19) - (22), represent the wave functions for the light quarks (u or d):

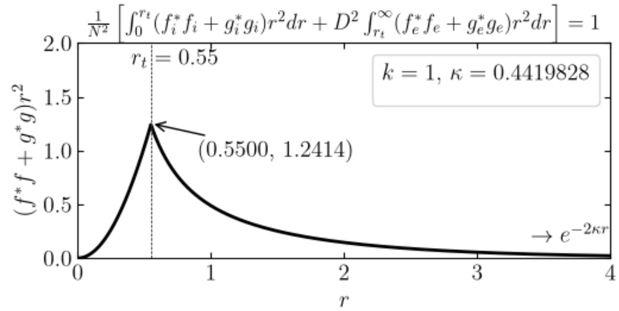

FIG. 1. Plot of $(f^*f + g^*g)r^2$ for $k = 1$, $\kappa = 0.4419828$ and $r_t = 0.5500$. The reason for this particular choice of k and κ is explained in subsection IV B. Note the equal and symmetric slop of the two rising and falling branches at r_t, where the Bessel first kinds are switched to the Bessel second kinds. Note the exponential decline of the outer branch to zero.

$$u_\uparrow(\mathbf{x}) \text{ or } d_\uparrow(\mathbf{x}) = \frac{e^{+i\varphi/2}}{\sqrt{4\pi}}\begin{bmatrix} f\sin\theta/2 \\ if\cos\theta/2 \\ ig\sin\theta/2 \\ g\cos\theta/2 \end{bmatrix}, \tag{28}$$

$$u_\downarrow(\mathbf{x}) \text{ or } d_\downarrow(\mathbf{x}) = \frac{e^{-i\varphi/2}}{\sqrt{4\pi}}\begin{bmatrix} f\cos\theta/2 \\ -if\sin\theta/2 \\ ig\cos\theta/2 \\ -g\sin\theta/2 \end{bmatrix}, \tag{29}$$

where $\mathbf{x} = (r, \theta, \phi)$ represents the three-dimensional spatial coordinates of a single quark.

Constructing the multi-particle wave function for a full nucleon requires careful consideration of quantum numbers. From standard textbooks on elementary particle physics [13], [14], [15] and [16], the total wave function of a baryon is the product of four components:

$$\psi(color)\psi(space)\psi(spin)\psi(flavor).$$

Because quarks are spin-1/2 fermions, the total wave function must be completely antisymmetric under the exchange of any pair of constituent quarks. To satisfy this requirement, the following constraints must be met:

> All physically observed hadrons are color singlets; hence, the $\psi(color)$ component is a singlet state that is completely antisymmetric under the exchange of any two quarks (an oscillator-based representation of quark colors can be found in [17]).
>
> The spatial component $\psi(space)$ can be treated as completely symmetric under particle exchange, assuming all three constituent quarks reside in their ground state with zero orbital angular momentum.

The spin component for the baryon decuplet ($j = 3/2$) is completely symmetric. However, for the baryon octet ($j = 1/2$), it possesses mixed symmetry. One must construct specific permutations—namely $\psi_{12}(spin)$, $\psi_{23}(spin)$, and $\psi_{13}(spin)$—each of which is antisymmetric under the exchange of its two designated indices $(1, 2, 3)$.

The flavor component follows an identical mixed-symmetry pattern, requiring the construction of $\psi_{12}(flavor)$, $\psi_{23}(flavor)$, and $\psi_{13}(flavor)$, all antisymmetric under the exchange of two of the three indices $(1, 2, 3)$.

When combined, these constraints dictate that the sum of the spin-flavor combinations must be totally symmetric under the permutations of the pair of indices (1,2), (2,3), and (1,3). For the baryon octet, this yields:

$$\begin{aligned}
&\psi(\text{baryon octet})\\
&\quad = \frac{\sqrt{2}}{3}\{\psi_{12}(\text{spin})\psi_{12}(\text{flavor})\\
&\qquad + \psi_{23}(\text{spin})\psi_{23}(\text{flavor})\\
&\qquad + \psi_{13}(\text{spin})\psi_{13}(\text{flavor})\}.
\end{aligned}$$

Substituting the explicit quark states from (28) and (29) into this template yields the explicit state for a proton with spin-up:

$$\begin{aligned}
\left|p;\frac{1}{2}\frac{1}{2}\right\rangle &= \frac{1}{3\sqrt{2}}\\
&\times \{2u_\uparrow(\mathbf{x}_1)u_\uparrow(\mathbf{x}_2)d_\downarrow(\mathbf{x}_3)\\
&\quad - u_\uparrow(\mathbf{x}_1)u_\downarrow(\mathbf{x}_2)d_\uparrow(\mathbf{x}_3)\\
&\quad - u_\downarrow(\mathbf{x}_1)u_\uparrow(\mathbf{x}_2)d_\uparrow(\mathbf{x}_3)\\
&+ 2u_\uparrow(\mathbf{x}_1)d_\downarrow(\mathbf{x}_2)u_\uparrow(\mathbf{x}_3)\\
&\quad - u_\downarrow(\mathbf{x}_1)d_\uparrow(\mathbf{x}_2)u_\uparrow(\mathbf{x}_3)\\
&\quad - u_\uparrow(\mathbf{x}_1)d_\uparrow(\mathbf{x}_2)u_\downarrow(\mathbf{x}_3)\\
&+ 2d_\downarrow(\mathbf{x}_1)u_\uparrow(\mathbf{x}_2)u_\uparrow(\mathbf{x}_3)\\
&\quad - d_\uparrow(\mathbf{x}_1)u_\downarrow(\mathbf{x}_2)u_\uparrow(\mathbf{x}_3)\\
&\quad - d_\uparrow(\mathbf{x}_1)u_\uparrow(\mathbf{x}_2)u_\downarrow(\mathbf{x}_3)\}. \quad (30)
\end{aligned}$$

The corresponding neutron wave function is obtained directly from (30) by swapping the u and d flavor labels while leaving all spin subscripts and spatial (x) designations unaltered.

IV. GRAVITATIONAL MANIFESTATION OF QUARKS AND NUCLEON

Quarks, as massive entities, curve their surrounding spacetime. For a nucleon composed of three valence quarks, the source term in (23) and (24) is tripled:

$$\alpha' = 3Kr\Big((f^*g' + fg'^*) - (f'^*g + f'g^*)\Big), \quad (31)$$

$$a' = -3 \times 2\omega Kr(f^*f + g^*g). \quad (32)$$

To justify the factor 3 above, we argue that the individual single-quark states $u(x)$ and $d(x)$ in (30) are mutually orthogonal to each other with no interactions among themselves.

A. Reduction of metric parameters $\alpha(r)$ and $a(r)$

For the interior region (${\alpha'}_i$ and α_i) using (A16) and (A17), the normalization constant N^2 included, yields:

$$\begin{aligned}
\alpha_i'(r) &= \frac{3}{N^2}Kr\Big((f_i^*g_i' + c.c.) - (f_i'^*g_i + c.c.)\Big)\\
&= \frac{3}{N^2}\Big(\frac{2}{K^2r}(-\kappa^2\cos 2kr + k^2\cosh 2\kappa r)\\
&\qquad + \frac{4k\kappa}{K^4r^2}(\kappa\sin 2kr - k\sinh 2\kappa r)\\
&\qquad - \frac{(k^2-\kappa^2)}{K^4r^3}(-\cos 2kr + \cosh 2\kappa r)\Big) r \le r_t,\\
&\Rightarrow 2K^2r \quad \text{as} \quad r \Rightarrow 0, \quad (33)
\end{aligned}$$

$$\begin{aligned}
&\alpha_i(r) = C_\alpha\\
&\quad + \frac{3}{N^2}\Bigg(\frac{1}{K^4r}\Big(k(k^2-5\kappa^2)\sin 2kr + \kappa(5k^2-\kappa^2)\sinh 2\kappa r\Big)\\
&\quad + \frac{(k^2-\kappa^2)}{2K^4r^2}(-\cos 2kr + \cosh 2\kappa r)\\
&\quad + 2\frac{(k^4 - 4k^2\kappa^2 + \kappa^4)}{K^4}\int(-\cos 2kr + \cosh 2\kappa r)\frac{dr}{r}\Bigg),\\
&\qquad r \le r_t. \quad (34)\\
&\Rightarrow C_\alpha + K^2r^2 \quad \text{as} \quad r \to 0,
\end{aligned}$$

where C_α is an integration constant that will be determined via boundary matching. For the exterior region (α_e' and α_e), (A18) and (A19), with N^2 and D^2 included, yields:

$$\begin{aligned}
\alpha_e'(r) &= \frac{3D^2}{N^2}Kr\Big((f_e^*g_e' + c.c.) - (f_e'^*g_e + c.c.)\Big)\\
&= \frac{3D^2}{N^2}\Big(\frac{4k^2}{K^2r} + \frac{8k^2\kappa}{K^4r^2} - \frac{2(k^2-\kappa^2)}{K^4r^3}\Big)e^{-2\kappa r},\\
&\qquad r \ge r_t. \quad (35)
\end{aligned}$$

$$\begin{aligned}
\alpha_e(r) = 1 + \frac{3D^2}{N^2}\Bigg(&e^{-2\kappa r}\Big(\frac{-2\kappa(5k^2-\kappa^2)}{K^4r} + \frac{(k^2-\kappa^2)}{K^4r^2}\Big)\\
&- \frac{4(k^4+\kappa^4-4k^2\kappa^2)}{K^4}\int e^{-2\kappa r}\frac{dr}{r}\Bigg),\\
&\qquad r \ge r_t. \quad (36)
\end{aligned}$$

For the exterior metric component α_e in (36), we set the integration constant to 1 to ensure that spacetime (α_e) becomes asymptotically flat at the spatial infinity.

In Equation (34) the interior integration constant C_α is subsequently adjusted so that $\alpha_i(r_t) = \alpha_e(r_t)$. Similarly, evaluating the metric component $a(r)$ from (A20) and (A21) yields:

$$\begin{aligned} a_i(r) = C_a + \frac{1}{N^2}\Bigg(& \frac{-6\omega}{2K^3 r}(k\sin 2kr + \kappa\sinh 2\kappa r) \\ & + \frac{6\omega}{4K^3 r^2}(-\cos 2kr + \cosh 2\kappa r) \\ & - \frac{6\omega k^2}{K^3}\int(-\cos 2kr + \cosh 2\kappa r)\frac{dr}{r}\Bigg), \quad r \le r_t. \end{aligned} \tag{37}$$

$$\begin{aligned} a_e(r) = 1 + \frac{6\omega D^2}{N^2}\Bigg(& e^{-2\kappa r}\left(\frac{\kappa}{K^3 r} + \frac{1}{2K^3 r^2}\right) \\ & + \frac{2(k^2 - 2\kappa^2)}{K^3}\int e^{-2\kappa r}\frac{dr}{r}\Bigg), \ r \ge r_t. \end{aligned} \tag{38}$$

In (38), the exterior integration constant is set to 1 to satisfy asymptotic flatness of a_e at infinity, while C_a in (37) is so chosen to guarantee that a remains strictly continuous at r_t.

In FIG. 2, we plot the metric coefficients α and a as functions of the radial distance r for the specific choice of $\omega \approx k = 1$ and $\kappa = 0.4419828$. The center is asymptotically flat, with deviations from flatness growing as r^2 as one moves away. Both metric coefficients (α and a) are smooth and continuous at r_t. At large radial distances, α and a decay exponentially to 1, returning smoothly to a flat spacetime.

FIG. 3 displays the squared metric components α^2 and a^2 as functions of r. The origin, where both parameters reach their global maxima, represents a point of unstable equilibrium. A massive quark may briefly linger around the center, but it will inevitably be driven outward by the repulsive general relativistic forces, $\propto \nabla(\alpha^2 - 1)$. On the other hand, the local minimum of α^2 at $r_c = 0.9704$ represents a point of stable equilibrium. The valence quarks will primarily dwell within this neighborhood, allowing r_c to be physically identified as the charge radius of the proton. Beyond r_c, the residual gravitational forces are minuscule and quickly vanish as $e^{-2\kappa r}$.

A noteworthy feature: singularities in gravitation, whether Newtonian or GR, stem from the point-particle assumption inherent in classical gravitating masses. Due to the extended nature of the spinor wave, there are no singularities in any of our spacetime metric coefficients.

A passing remark of interest for researchers in alternative gravitions and dark matter scenarios: at sufficiently large distances, the gravitational force is

$$\begin{aligned} \frac{1}{2}\frac{d}{dr}(\alpha_e^2 - 1) &= \alpha_e\alpha_e' \approx \alpha_e' \\ &= \frac{3D^2}{N^2}\left(\frac{4k^2}{K^2 r} + \frac{8k^2\kappa}{K^4 r^2} - \frac{2(k^2-\kappa^2)}{K^4 r^3}\right)e^{-2\kappa r}. \end{aligned}$$

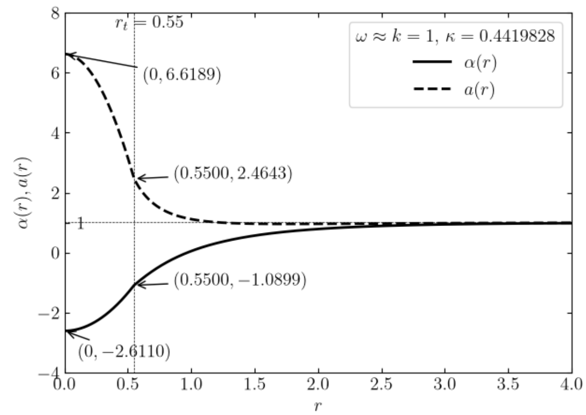

FIG. 2. Plots of $\alpha(r)$ and $a(r)$ as functions of r for $\omega \approx k = 1$ and $\kappa = 0.4419828$. In determining the transition radius, $r_t = 0.5500$, we required the first derivatives of the inner and outer α and a to be continuous. When adjusting the integration constants, C_α and C_a, we ensured that the inner and outer α and a functions are also continuous. Both α and a approach 1 as $r \to \infty$, indicating that the spacetime is asymptotically flat at infinity. The falloff to 1 is exponential, governed by $e^{-2\kappa r}$. The center is also flat; both α and a approach constants as $r \to 0$. Deviations from flatness grow as r^2 and higher even powers of r.

Setting aside the exponential factor $e^{-2\kappa r}$, the r^{-2} term should be identified with the Newtonian force. The r^{-1} and r^{-3} terms are non-Newtonian and non-GR forces. At far distances, the r^{-1} force declines much more slowly than the other two. Now consider a galaxy composed of about 10^{70} to 10^{72} protons and neutrons. The accumulated r^{-1} forces of such huge number of atoms and molecules would have sufficient magnitude to explain the flat rotation curves of spiral galaxies and the Tully-Fisher relation, see [18] for a similar phenomenon in a galaxy composed of Klein-Gordon particles.

B. Inner Dynamics of Nucleons-Determination of κ

In FIG. 3, from the center up to r_c, the negative slope of α^2 represents the outward force on quarks. From r_c to infinity, the slope becomes positive and the force turns to be inward. To achieve equilibrium, the outward and inward forces must balance each other. This is the origin of von Laue's condition for the dynamical stability of nucleons, which is discussed below.

The negative and complexified version of (9) defines the internal pressure profile $P(r)$ within the nucleon:

$$P(r) = -S^r_r = \frac{1}{4\pi}(f^* g' - f'^* g) + c.c. = -\frac{1}{12\pi}\frac{\alpha'}{Kra} \tag{39}$$

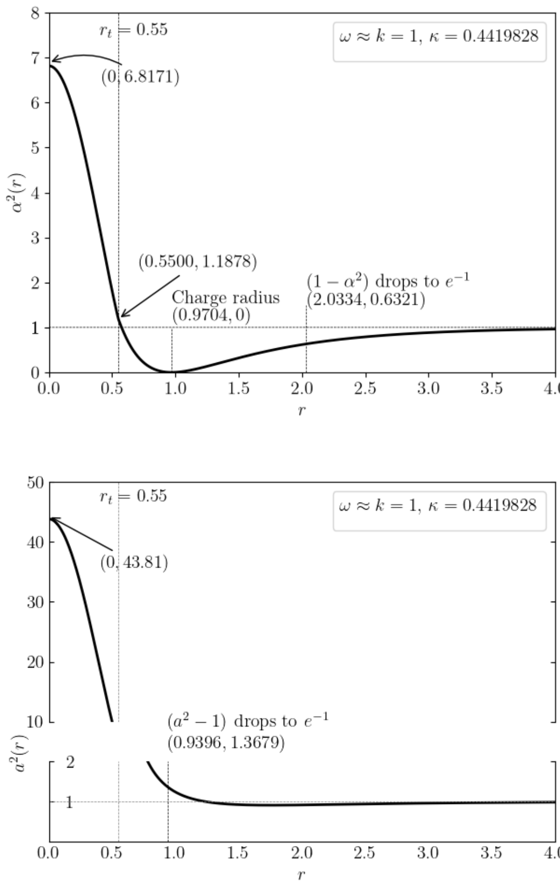

FIG. 3. Plots of $\alpha^2(r)$ and $a^2(r)$ for $\omega \approx k = 1$ and $\kappa = 0.4419828$. The center, where both functions reach their maxima, is a point of unstable equilibrium. A massive quark may linger there briefly but will eventually be driven away by gravitational forces. The minimum of α^2 at $r_c = 0.9704$ represents a stable point of equilibrium, meaning quarks will primarily dwell in that neighborhood. Consequently, it is appropriate to define r_c as the charge radius of the nucleon. Beyond r_c, minute gravitational forces persist but die away exponentially as $e^{-2\kappa r}$.

Van Laue's theorem for static nucleon stability [19] requires the integrated pressure over all space to vanish

$$\int P\sqrt{-g}dr = 0, \qquad \sqrt{-g} = \sqrt{\alpha^2 a^2}r^2\sin\theta.$$

This condition, however, cannot be satisfied for arbitrary choices of (k and κ). In this work, we fix the dimensionless parameter $k = 1$, and via numerical root-finding, determine the required value of κ to satisfy van Laue criterion. We find:

$$\begin{aligned} &k = 1, \quad \kappa = 0.4419828, \\ &\int P\sqrt{-g}drd\theta d\phi = \frac{-1}{3K}\left(\int_0^{r_c}\alpha\alpha' r dr + \int_{r_c}^{\infty}\alpha\alpha' r dr\right) \\ &\quad = 0.287749302 - 0.287749751 = -0.45\times 10^{-7}. \end{aligned} \tag{40}$$

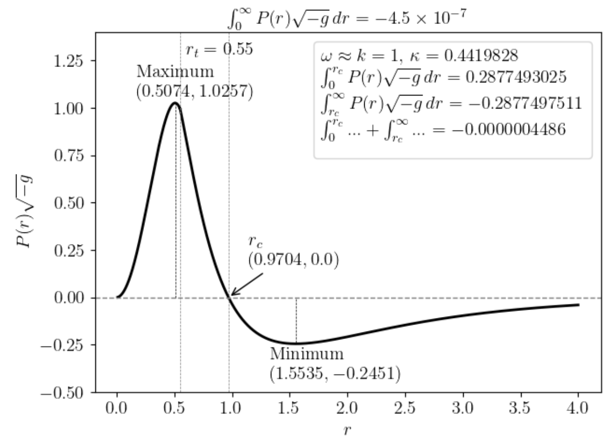

FIG. 4. Plot of $P\sqrt{-g}$ as a function of radius. The values on the curve are in dimensionless Planck units. For example, the maximum outward force of 1.0257 in Planck units at $r = 0.5074$ corresponds to $1.24\times 10^{44} Pa.m^2(N)$ (see the main text for the conversion from Planck to SI units).

Our numerical calculations satisfy van Laue's condition to an accuracy of approximately 4.5×10^{-8}. Higher numerical precision can be achieved with finer grid resolution.

FIG. 4 is a plot of $P\sqrt{-g}$ as a function of r. The dimensionless numbers there are in Planck units. For physical clarity, we provide two examples converting these values to the International System of Units (SI):

1) The peak value in FIG. 4, 1.0257, carries the dimensions of pressure times area (force). Its SI equivalent is calculated as:

$$\begin{aligned} &1.0257\times(4.63\times 10^{113})\times(1.62\times 10^{-35})^2 \\ &\qquad = 1.24\times 10^{44}\ Pa.m^2(N), \end{aligned}$$

where the first term in parentheses represents the SI equivalent of the Planck unit of pressure and the second represents SI equivalent of the Planck area.

2) The value 0.2877 in FIG. 4 has dimensions of volume times pressure (energy). Its SI equivalent is given by:

$$\begin{aligned} &0.2877\times(4.63{\times}10^{113})\times(1.62\times 10^{-35})^3 \\ &\qquad = 5.66\times 10^{8}\ Pa.m^3(N.m), \end{aligned} \tag{41}$$

Nuclear physicists generally agree that the internal pressures acting inside a nucleon exceed those within core neutron stars by many orders of magnitude—typically reaching 10^{35} Pa inside nucleons compared to roughly 5×10^8 Pa in neutron stars [20], [21], [22]. The ultra-high internal forces derived from our general relativistic framework are fully consistent with these established nuclear property estimates.

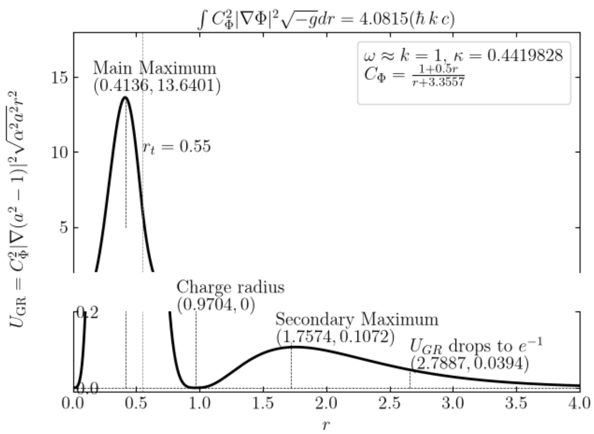

FIG. 5. Distribution of the (emergent) GR energy of a nucleon, derived from general relativistic and quantum considerations. The energy density is zero at the center, reaches its maximum at $r = 0.4136$, drops to zero at the charge radius $r_c = 0.9704$, is followed by a negligible secondary maximum at 1.7574, and eventually decays exponentially to zero at infinity.

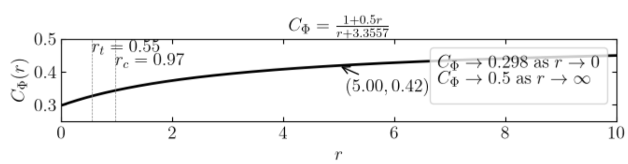

FIG. 6. Plot of $C_\Phi = \frac{1+0.5r}{r+3.3557}$

C. General Relativistic energy density inside nucleons

General relativity is fundamentally a tensor field theory characterized by significant mathematical subtleties. However, to illustrate the physical mechanism clearly, we adopt a simplified Newtonian perspective. We argue that the term $\Phi(r) = (\alpha^2 - 1)$, when scaled by an appropriate factor C_Φ, functions as an effective Newtonian gravitational potential field. Associated with Φ is a gravitational force field $\nabla\Phi$ and a corresponding gravitational potential energy density proportional to $\frac{1}{2}|\nabla\Phi|^2$. In the weak-field limit at large radial distances r, the scaling factor C_Φ naturally approaches the Newtonian case, $\frac{1}{2}$. Inside the ultra-dense core of a nucleon, its precise functional form is less certain. We model $C_\Phi(r)$ as a slowly varying function r, that approaches a finite constant at the origin and asymptotically levels out to $\frac{1}{2}$ at infinity. We then use experimentally measured nucleon parameters to calibrate its value at the origin, $C_\Phi(0)$.

There is another issue to clarify. Up to this stage, the parameter k has been treated as a dimensionless unit ($k = 1$). To map this model onto real physical systems, we must determine its actual physical dimensional value.

Thus, to fix the two remaining unknowns—the $C_\Phi(0)$ and the physical scale of k—we calibrate our model against two established laboratory measurements:

1. The emergent mass-energy of a nucleon (the total mass minus the baseline Higgs-induced rest masses of its three valence quarks), which set it ≈ 929 Mev.

2. The universally accepted physical charge radius of the proton, which is roughly 0.84 fm.

By evaluating the integrated general relativistic energy U_{GR} and the charge radius r_c over a range of trial parameters, we converge on the following specific profile through numerical optimization:

$$C_\Phi(r) = \frac{1 + 0.5r}{3.3557 + r} \to 0.298 \text{ as } r \to 0, \ \to 0.5 \text{ as } r \to \infty.$$

The functional behavior of C_Φ is illustrated in FIG. 6. The total integrated general relativistic potential energy and the physical value of the wave vector k are determined to be:

$$U_{GR} = \int C_\Phi^2 |\nabla\Phi|^2 \sqrt{-g} dr = 2 \int C_\Phi^2 \alpha^3 \alpha'^2 a r^2 dr$$
$$= 4.081(\hbar k c) = 929 \text{ Mev}, \tag{42}$$
$$k = 1.1533 \text{ fm}^{-1}, \quad k^{-1} = r_{nuc} = 0.867 \text{ fm}. \tag{43}$$

Setting $r_{nuc} = 0.867$ fm scales all dimensionless radial distances down by a physical factor of 1.1533. These calibrated physical parameters are summarized in Table 1.

k dimensionless: 1,
k dimensional: $1.1533\,\mathrm{fm}^{-1}$, U_{GR}: $929\,\mathrm{MeV}$

distance	dimensionless	dimensional
main max. U_{GR}	0.4136	0.3586 fm
r_t transition	0.5500	0.4769 fm
r_c charge radius	0.9704	0.8414 fm
2^{nd} max. U_{GR}	1.7574	1.5238 fm
U_{GR} drops to e^{-1}	2.7887	2.4180 fm

TABLE I. Summary of the calibrated nucleon model parameters

It is important to note that, the integrated GR energy in FIG. 5, the dimensionless number 4.0815, represents the total quantum mechanical energy of quarks expressed in units of $\hbar\omega \approx \hbar kc$ (the total energy of a single valence quark). The integrated energy in (42) represents a purely emergent mass-energy, which is conceptually distinct from the Higgs-induced rest masses of the valence quarks. Had we a quantised theory of general relativity, this energy U_{GR} would represent a description of localized gravitons mediating the strong gravitational field—acting as the general relativistic counterparts to the gluons of quantum chromodynamics (QCD).

The spatial distribution of this emergent energy is plotted in FIG. 5. It leads to several key physical conclusions:

a. The Origin ($r = 0$): The center represents a state of maximum general relativistic potential ($\Phi = C_\Phi(r)(\alpha^2 - 1)$ where the gradient vanishes ($\nabla\Phi = 0$). Consequently, there are no localized gravitational forces or emergent energy densities at the exact origin, making it a point of unstable equilibrium. Moving outward, the non-zero gradient causes the general relativistic energy density to rise rapidly.

b. The Mass Center ($r \approx 0.4136$): The field gradient and energy density reach their global maxima at this radius. This position can be interpreted as the physical center-of-mass of the nucleon structure.

c. The Stable point ($r = 0.9704$): At this minimum, both the general relativistic force and energy density drop to zero, creating a stable potential well. Quarks are naturally driven toward this radius, concentrating their electromagnetic signatures here. This matches what experimental particle physicists measure as the proton's charge radius (0.8414 fm).

d. The Exterior Cloud ($r \approx 1.7574$): Beyond the stable minimum, the system exhibits a minor secondary energy maximum, indicating a diffuse cloud of general relativistic energy around the outer edge before it decays exponentially to zero.

D. Finally Asymptotic Freedom and Confinement

As already mentioned, the center is an unstable equilibrium point. There the general relativistic forces vanish. Similarly, the stable charge radius r_c represents a zero-force environment. Quarks are free to move within this force-free corridor around the charge radius, providing a natural explanation for the phenomenon of *asymptotic freedom*. Concurrently, they are strictly *confined* to this localized domain (r_c) because their quantum probability density drops exponentially to zero outside this zone, preventing them from escaping into free space.

E. Digression: Findings of $J/\Psi - 007$ Collaboration

The J/Ψ particle is a charmonium meson with a mass of 3.097 GeV and an exceptionally short mean lifetime of 7.2×10^{-20} seconds. It was discovered independently in 1974 by a SLAC team led by Burton Richter [23], [24] and a BNL team (Brookhaven National Laboratory) led

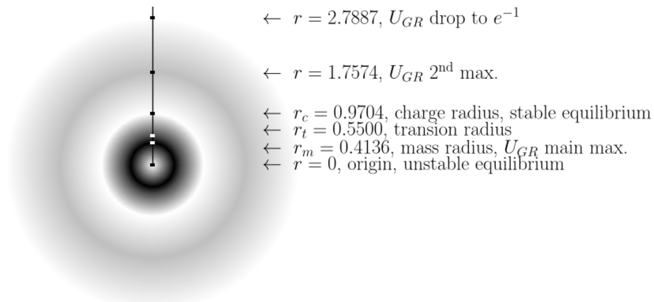

FIG. 7. Nucleon's emergent GR energy distribution. Same data as in FIG. 5. The darker a region the larger the GR energy density. The center, painted white, is an unstable point with no GR forces or energies there. The darkest wide ring around $r = 0.4136$, is the region of highest energy density. On moving out, darkness fades away and eventually gives way to the whitish ring at about $r \approx 0.9704$. This is the stable region. Quarks are driven to that vicinity and exhibit enhanced electromagnetic behaviors. The Particle Physics Community has, appropriately, named $r = 0.9704$ as the charge radius of the proton. Beyond the charge radius there is the secondary maximum at about $r = 1.7574$, with a dilute GR energy. It, however, phases out exponentially as $e^{-2\kappa r}$.

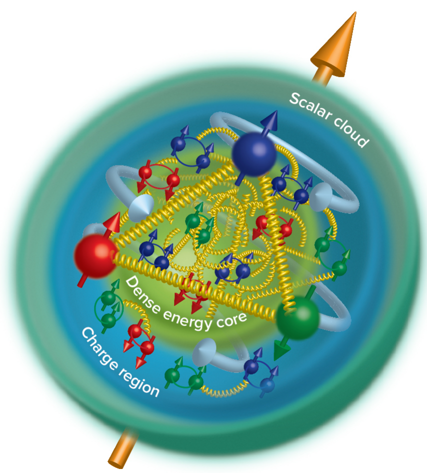

FIG. 8. The proton mass radius is smaller than the electric charge radius (a dense core), while a cloud of scalar gluon activity extends beyond the charge radius. This finding could shed light on confinement and the mass distribution in the proton. (Image and legend by Argonne national Laboratory)

by Samuel Ting [25].. A recent experimental collaboration between Jefferson Lab and Argonne National Laboratory—the $J/\Psi - 007$ project—has provided insights into the origin of the emergent mass generated by gluons inside the proton [26], [27], [28], [29], [30], [31], [32], [33], [34], [35], [36], [37], [38], [39], [40]. Key conclusions from the Jefferson Lab press release include:

1 $\cdots$ *Nuclear physicists may have finally pinpointed where in the proton a large fraction of its mass re-*

sides. ⋯ the mass that is generated by the proton's gluons. ⋯

2 ⋯ *The radius of this mass structure is smaller than the charge radius, and so it kind of gives us a sense of the hierarchy of the mass versus the charge structure of the nucleon," said experiment co-spokesperson Mark Jones, ⋯* [41], [42], [43]

3 ⋯ *the experimenters determined the aforementioned gluonic mass radius dominated by graviton-like gluons, as well as a larger radius of attractive scalar gluons that extend beyond the moving quarks and confine them.*

4 ⋯ *One of the more puzzling findings from our experiment is that in one of the theoretical model approaches, our data hint at a scalar gluon distribution that extends well beyond the electromagnetic proton radius, Joosten said.*

These four experimental discoveries directly mirror the four theoretical insights (*a*–*d*) derived from our general relativistic model (subsection IV C):

Both the $J/\Psi - 007$ collaboration and our model conclude that the bulk of the proton's total mass is purely emergent—attributed to tensor-like gluons in QCD and to general relativistic gravitational energy in our framework. In a would be unified quantum gravity theory, these descriptions would be mathematically equivalent.

Both approaches agree that the mass radius of the proton is significantly smaller than its electric charge radius (4.6 fm in our model).

The $J/\Psi - 007$ collaboration identifies a diffuse scalar gluon cloud extending past the charge boundary, which matches the exterior general relativistic energy cloud derived in our framework.

V. CONCLUDING REMARKS

In this paper, we have modeled quarks as *normalizable* Dirac spinors that possess sufficient mass-energy to dynamically curve their surrounding spacetime. To ensure square-integrability of the spinors over all space, we introduced a complex-valued wave propagation vector via a Yukawa-like amelioration scheme. Assuming a static, spherically symmetric spacetime metric, we find that:

Thanks to the wave nature of spinors, there is no singularity in the resulting spacetime. This is to be contrasted with singularities of Schwarzschild's spacetime or others.

Inside the nucleon, spacetime is flat at the origin, with metric deviations growing as even powers of the radial distance (r).

Outside the nucleon the spacetime is asymptotically flat. The metric coefficients α and a tend to 1 as $r \to \infty$.

There are two distinct equilibrium points to the spacetime, defined by the extrema of α^2 and a^2: an unstable point at the origin ($r = 0$), an almost parabolic stable potential well around the charge radius (r_c).

Quarks occupy the force-free environment of the stable charge radius. While asymptotically free, their confinement is enforced by the exponential decay of their wave density outside this zone.

Eventually, we have demonstrated a direct structural correspondence between our general relativistic model of nucleons and the experimental mass profiles published by the $J/\Psi - 007$ collaboration.

Far out a nucleon, there are r^{-1}, r^{-2}, r^{-3} forces. The first one may be of interest to those who may fancy to explain the Tully-Fisher relation, the flat rotation curves of spiral galaxies.

We acknowledge that treating $C_\Phi(r)(\alpha^2 - 1)$ as an effective Newtonian potential in Section IV C is a simplifying approximation that may draw scrutiny from general relativity purists.

Nonetheless, this work demonstrates that the general relativistic forces at the femtometer scale is remarkably strong and capable of replicating the known features of the strong force. This suggests that the fundamental interactions of nature might ultimately be classified into just two categories: the electroweak and the gravostrong forces.

Acknowledgment: We express our sincere gratitude to Professor Kazem Azizi for his invaluable expert advice, guidance, and suggestions during the conceptual development of this paper.

Appendix

$$\cos Kz^* \cos Kz = \frac{1}{2}(\cos 2kr + \cosh 2\kappa r), \tag{A1}$$

$$\sin Kz^* \sin Kz = \frac{1}{2}(-\cos 2kr + \cosh 2\kappa r), \tag{A2}$$

$$\sin Kz^* \cos Kz = \frac{1}{2}(\sin 2kr - i \sinh 2\kappa r), \tag{A3}$$

$$\sin Kz \cos Kz^* = \frac{1}{2}(\sin 2kr + i \sinh 2\kappa r), \tag{A4}$$

$$f_i = \frac{\sin Kz}{Kz}, \qquad g_i = -\frac{K_-}{K}\left(\frac{\cos Kz}{Kz} - \frac{\sin Kz}{K^2 z^2}\right),$$

$$f_e = \frac{e^{iKz}}{Kz}, \qquad g_e = -\frac{K_-}{K} e^{iKz}\left(\frac{i}{Kz} - \frac{1}{K^2z^2}\right).$$

$$f_i' = K_+\left(\frac{\cos Kz}{Kz} - \frac{\sin Kz}{K^2z^2}\right),$$
$$g_i' = K\left(\frac{\sin Kz}{Kz} + 2\frac{\cos Kz}{K^2z^2} - 2\frac{\sin Kz}{K^3z^3}\right),$$

$$f_e' = K_+ e^{iKz}\left(\frac{i}{Kz} - \frac{1}{K^2z^2}\right),$$
$$g_e' = K e^{-iKz}\left(\frac{1}{Kz} + \frac{3i}{K^2z^2} - \frac{4}{K^3z^3}\right).$$

$$\begin{aligned} f_i^* f_i' + c.c &= \frac{1}{K^2r^2}(k\sin 2kr + \kappa\sinh 2\kappa r) \\ &\quad - \frac{1}{K^2r^3}(-\cos 2kr + \cosh 2\kappa r), \\ g_i^* g_i' + c.c. &= \frac{1}{K^2r^2}(-k\sin 2kr + \kappa\sinh 2\kappa r) \\ &\quad - \frac{1}{K^4r^3}\Big((3k^2+\kappa^2)\cos 2kr + (k^2+3\kappa^2)\cosh 2\kappa r\Big) \\ &\quad + \frac{4}{K^4r^4}(k\sin 2kr + \kappa\sinh 2\kappa r) \\ &\quad - \frac{2}{K^4r^5}(-\cos 2kr + \cosh 2\kappa r). \end{aligned}$$

$$\begin{aligned} f_i^* f_i' + g_i^* g_i' + c.c. &= \frac{2\kappa}{K^2r^2}\sinh 2\kappa r \\ &\quad - \frac{2}{K^4r^3}\Big(k^2\cos 2kr + (k^2+2\kappa^2)\cosh 2\kappa r\Big) \\ &\quad + \frac{4}{K^4r^4}(k\sin 2kr + \kappa\sinh 2\kappa r) \\ &\quad - \frac{2}{K^4r^5}(-\cos 2kr + \cosh 2\kappa r). \end{aligned}$$

$$f_e^* f_e' + c.c. = -2e^{-2\kappa r}\left(\frac{\kappa}{K^2r^2} + \frac{1}{K^2r^3}\right),$$
$$g_e^* g_e' + c.c. = -2e^{-2\kappa r}\left(\frac{\kappa}{K^2r^2} + \frac{1}{K^2r^3} - \frac{4\kappa}{K^4r^4} + \frac{2}{K^4r^4}\right).$$

$$\begin{aligned} &f_e^* f_e' + g_e^* g_e' + c.c. \\ &\quad = -4e^{-2\kappa r}\left(\frac{\kappa}{K^2r^2} + \frac{1}{K^2r^3} - \frac{2\kappa}{K^4r^4} + \frac{1}{K^4r^5}\right). \end{aligned}$$

$$f_i^* f_i = \frac{1}{2K^2r^2}(-\cos 2kr + \cosh 2\kappa r), \tag{A5}$$
$$\begin{aligned} g_i^* g_i &= \frac{1}{2K^2r^2}(\cos 2kr + \cosh 2\kappa r) \\ &\quad - \frac{1}{K^4r^3}(k\sin 2kr + \kappa\sinh 2\kappa r) \\ &\quad + \frac{1}{2K^4r^4}(-\cos 2kr + \cosh 2\kappa r). \end{aligned} \tag{A6}$$

$$\begin{aligned} f_i^* g_i + c.c. &= -\frac{1}{K^3r^2}(k\sin 2kr - \kappa\sinh 2\kappa r) \\ &\quad - \frac{(k^2-\kappa^2)}{K^5r^3}(\cos 2kr - \cosh 2\kappa r). \end{aligned} \tag{A7}$$

$$f_e^* f_e = \frac{e^{-2\kappa r}}{K^2r^2}. \tag{A8}$$
$$g_e^* g_e = e^{-2\kappa r}\left(\frac{1}{K^2r^2} + \frac{2\kappa}{K^4r^3} + \frac{1}{K^4r^4}\right). \tag{A9}$$

$$f_e^* g_e + c.c. = -2e^{-2\kappa r}\left(\frac{\kappa}{K^3r^2} + \frac{(k^2-\kappa^2)}{K^5r^3}\right). \tag{A10}$$

Calculation of D^2 and N^2: From (A5) - (A9), one has,

$$\begin{aligned} (f_i^* f_i + g_i^* g_i) &= \frac{\cosh 2\kappa r}{K^2r^2} - \frac{(k\sin 2kr + \kappa\sinh 2\kappa r)}{K^4r^3} \\ &\quad + \frac{(-\cos 2kr + \cosh 2\kappa r)}{2K^4r^4}, \end{aligned} \tag{A11}$$
$$(f_e^* f_e + g_e^* g_e) = e^{-2\kappa r}\left(\frac{2}{K^2r^2} + \frac{2\kappa}{K^4r^3} + \frac{1}{K^4r^4}\right), \tag{A12}$$

$$D^2 = (f_i^* f_i + g_i^* g_i)_{r_t} / (f_e^* f_e + g_e^* g_e)_{r_t}. \tag{A13}$$

$$\begin{aligned} N^2 &= \int_0^{r_t} (f_i^* f_i + g_i^* g_i)\, r^2 dr \\ &\quad + D^2 \int_{r_t}^{\infty} (f_e^* f_e + g_e^* g_e)\, r^2 dr \\ &= \left(\frac{\sinh 2\kappa r_t}{2\kappa K^2} - \frac{(\cosh 2\kappa r_t - \cos 2kr_t)}{2K^4 r_t}\right) \\ &\quad + \frac{D^2}{\kappa K^2} e^{-2\kappa r_t}\left(1 + \frac{\kappa}{K^2 r_t}\right). \end{aligned} \tag{A14}$$

Calculation of α_i' and α_i for $r \le r_t$:

$$\alpha' = 3Kr\left[(f^* g' + c.c.) - (f'^* g + c.c.)\right].$$

$$
\begin{aligned}
(f_i^* g_i{}' + c.c.) &= \\
&= \frac{1}{Kr^2}(-\cos 2kr + \cosh 2\kappa r) \\
&\quad + \frac{2}{K^3 r^3}(k \sin 2kr - \kappa \sinh 2\kappa r) \\
&\quad - \frac{2(k^2-\kappa^2)}{K^5 r^4}(-\cos 2kr + \cosh 2\kappa r). \\
(f_i'^* g_i + c.c.) &= \\
&= -\frac{(k^2-\kappa^2)}{K}\bigg(\frac{1}{K^2 r^2}(\cos 2kr + \cosh 2\kappa r) \\
&\quad - \frac{2}{K^4 r^3}(k \sin 2kr + \kappa \sinh 2\kappa r). \\
&\quad + \frac{1}{K^4 r^4}(-\cos 2kr + \cosh 2\kappa r)\bigg).
\end{aligned}
\tag{A15}
$$

$$
\begin{aligned}
\alpha_i'(r) = 3\bigg(&\frac{2}{K^2 r}(-\kappa^2 \cos 2kr + k^2 \cosh 2\kappa r) \\
&+ \frac{4k\kappa}{K^4 r^2}(\kappa \sin 2kr - k \sinh 2\kappa r) \\
&- \frac{(k^2-\kappa^2)}{K^4 r^3}(-\cos 2kr + \cosh 2\kappa r)\bigg) \\
&\to r \text{ as } r \to 0.
\end{aligned}
\tag{A16}
$$

$$
\begin{aligned}
&\alpha_i(r) = \\
&3\bigg(\frac{1}{K^4 r}\Big(k(k^2-5\kappa^2)\sin 2kr + \kappa(5k^2-\kappa^2)\sinh 2\kappa r\Big) \\
&+ \frac{(k^2-\kappa^2)}{2K^4 r^2}(-\cos 2kr + \cosh 2\kappa r) \\
&- 2\frac{(k^4 - 4k^2\kappa^2 + \kappa^4)}{K^4}\int(\cos 2kr - \cosh 2\kappa r)\frac{dr}{r}\bigg),
\end{aligned}
\tag{A17}
$$

Integration constant to be added.

Calculation of α_e' and α_e for $r \geq r_t$:

$$
\begin{aligned}
&(f_e{}^* g_e' + c.c.) \\
&\quad = 2e^{-2\kappa r}\left(\frac{1}{Kr^2} + \frac{2\kappa}{K^3 r^3} - \frac{2(k^2-\kappa^2)}{K^5 r^4}\right). \\
&(f_e'^* g_e + c.c.) \\
&\quad = -2\frac{(k^2-\kappa^2)}{K^2}e^{-2\kappa r}\left(\frac{1}{Kr^2} + \frac{2\kappa}{K^3 r^3} + \frac{1}{K^3 r^4}\right).
\end{aligned}
$$

$$
\begin{aligned}
\alpha_e'(r) &= 3Kr\Big((f_e^* g_e' + c.c.) - (f_e'^* g_e + c.c.)\Big) \\
&= 6e^{-2\kappa r}\left(\frac{2k^2}{K^2 r} + \frac{4k^2\kappa}{K^4 r^2} - \frac{(k^2-\kappa^2)}{K^4 r^3}\right).
\end{aligned}
\tag{A18}
$$

$$
\begin{aligned}
\alpha_e(r) = 3\bigg(&e^{-2\kappa r}\Big(\frac{-2\kappa(5k^2-\kappa^2)}{K^4 r} + \frac{(k^2-\kappa^2)}{K^4 r^2}\Big) \\
&- \frac{4(k^4+\kappa^4-4k^2\kappa^2)}{K^4}\int e^{-2\kappa r}\frac{dr}{r}\bigg),
\end{aligned}
\tag{A19}
$$

Integration constant to be added.

Calculation of a_i and a_e

$$
\begin{aligned}
a_i' &= -3\omega Kr(f_i^* f_i + g_i^* g_i) \\
&= -3\omega Kr\bigg(-\Big(\frac{k \sin 2kr}{K^4 r^2} + \frac{\cos 2kr}{2K^4 r^3}\Big) \\
&\qquad + \Big(\frac{\cosh 2\kappa r}{K^2 r} - \frac{\kappa \sinh 2\kappa r}{K^4 r^2} + \frac{\cosh 2\kappa r}{2K^4 r^3}\Big)\bigg) \\
a_i &= -\frac{6\omega}{2K^3 r}(k \sin 2kr + \kappa \sinh 2\kappa r) \\
&\quad + \frac{6\omega}{4K^3 r^2}(-\cos 2kr + \cosh 2\kappa r) \\
&\quad - \frac{6\omega k^2}{K^3}\int(-\cos 2kr + \cosh 2\kappa r)\frac{dr}{r},
\end{aligned}
\tag{A20}
$$

Integration constant to be added.

$$
\begin{aligned}
a_e' &= -3\omega Kr e^{-2\kappa r}\left(\frac{2}{K^2 r^2} + \frac{2\kappa}{K^4 r^3} + \frac{1}{K^4 r^4}\right) \\
a_e &= -3\omega K\int(f_e^* f_e + g_e^* g_e) r\,dr \\
&= 1 + 6\omega\bigg(e^{-2\kappa r}\Big(\frac{\kappa}{K^3 r} + \frac{1}{2K^3 r^2}\Big) \\
&\quad + \frac{2(k^2-2\kappa^2)}{K^3}\int e^{-2\kappa r}\frac{dr}{r}\bigg).
\end{aligned}
\tag{A21}
$$

Integration constant to be added.

[1] V. Fock, Zeitschrift für Physik **57**, 261 (1929).

[2] V. Fock and D. Ivanenko, Zeitschrift für Physik **54**, 798 (1929).

[3] H. Nieh and M. Yan, Annals of Physics **138**, 237 (1982).

[4] V. Bargmann, Sitzungsberichte der Preussischen Akademie der Wissenschaften. Physikalisch-mathematische Klasse **1**, 346 (1932).

[5] E. Schrödinger, Phys.Math. Kl. , 105 (1932).

[6] R. Ruffini and S. Bonazzola, Physical Review **187**, 1767 (1969).

[7] A. Ferrari and R. Ruffini, Physical Review **187**, 1767 (1969).

[8] R. Brito, V. Cardoso, C. A. Herdeiro, and E. Radu, Physics Letters B **752**, 291 (2016).

[9] C. A. Herdeiro and E. Radu, Symmetry **12**, 2032 (2020).

[10] E. Daka, N. N. Phan, and B. Kain, Physical Review D **100**, 084042 (2019).

[11] M. Alcubierre, The dirac equation in general relativity and the 3+1 formalism (2025), arXiv:2503.03918 [gr-qc].

[12] Y. Sobouti, Quantum Studies: Mathematics and Foundations **10**, 223 (2023).

[13] D. Griffiths, *Introduction to elementary particles* (John Wiley & Sons, 2020).

[14] C. Itzykson and J.-B. Zuber, *Quantum Field Theory* (McGraw-Hill, New York, 1980).

[15] J. D. Bjorken and S. D. Drell, *Relativistic Quantum Mechanics* (McGraw-Hill, New York, 1964).

[16] M. E. Peskin and D. V. Schroeder, *An Introduction to Quantum Field Theory* (Addison-Wesley, Reading, MA, 1995).

[17] Y. Sobouti, Journal of Physics Communications **2**, 085006 (2018).

[18] Y. Sobouti and H. Sheikhahmadi, Modern Physics Letters A **40**, 2450215 (2025).

[19] M. Laue, Annalen der Physik **340**, 524 (1911).

[20] V. Burkert, L. Elouadrhiri, and F. Girod, Nature **557**, 396 (2018).

[21] Z. Dehghan, F. Almaksusi, and K. Azizi, Journal of High Energy Physics **2025**, 1 (2025).

[22] M. Goharipour, H. Hashamipour, H. Fatehi, F. Irani, K. Azizi, S. Goloskokov, and M. Collaboration), Physical Review D **112**, 014016 (2025).

[23] J.-E. Augustin, A. M. Boyarski, M. Breidenbach, F. Bulos, J. Dakin, G. Feldman, G. Fischer, D. Fryberger, G. Hanson, B. Jean-Marie, *et al.*, Physical Review Letters **33**, 1406 (1974).

[24] J.-J. Aubert, U. Becker, P. Biggs, J. Burger, M. Chen, G. Everhart, P. Goldhagen, J. Leong, T. McCorriston, T. Rhoades, *et al.*, Physical Review Letters **33**, 1404 (1974).

[25] S. Ting, Nuclear Physics B , 117014 (2025).

[26] Y. Hatta, A. Rajan, and D.-L. Yang, Physical Review D **100**, 014032 (2019).

[27] P. Sun, X.-B. Tong, and F. Yuan, Physics Letters B **822**, 136655 (2021).

[28] K. A. Mamo and I. Zahed, Physical Review D **103**, 094010 (2021).

[29] Y. Guo, X. Ji, and Y. Liu, Physical Review D **103**, 096010 (2021).

[30] D. E. Kharzeev, Physical Review D **104**, 054015 (2021).

[31] K. A. Mamo and I. Zahed, Physical Review D **106**, 086004 (2022).

[32] B. Duran, Z.-E. Meziani, S. Joosten, M. Jones, S. Prasad, C. Peng, W. Armstrong, H. Atac, E. Chudakov, H. Bhatt, *et al.*, Nature **615**, 813 (2023).

[33] S. Adhikari, F. Afzal, C. Akondi, M. Albrecht, M. Amaryan, V. Arroyave, A. Asaturyan, A. Austregesilo, Z. Baldwin, F. Barbosa, *et al.*, Physical Review C **108**, 025201 (2023).

[34] D. C. Hackett, D. A. Pefkou, and P. E. Shanahan, Physical Review Letters **132**, 251904 (2024).

[35] Z.-E. Meziani, arXiv preprint arXiv:2403.08423 (2024).

[36] S. Joosten, Z.-E. Meziani, S. Prasad, J. Swartz, B. Duran, M. K. Jones, H. Klest, M. Paolone, C. Peng, W. Armstrong, *et al.*, arXiv preprint arXiv:2602.14416 (2026).

[37] H.-W. Lin, E. R. Nocera, F. Olness, K. Orginos, J. Rojo, A. Accardi, C. Alexandrou, A. Bacchetta, G. Bozzi, J.-W. Chen, *et al.*, Progress in Particle and Nuclear Physics **100**, 107 (2018).

[38] M. Constantinou, A. Courtoy, M. A. Ebert, M. Engelhardt, T. Giani, T. Hobbs, T.-J. Hou, A. Kusina, K. Kutak, J. Liang, *et al.*, Progress in Particle and Nuclear Physics **121**, 103908 (2021).

[39] S. Forte and G. Watt, Annual Review of Nuclear and Particle Science **63**, 291 (2013).

[40] A. Accardi, A. Bacchetta, L. Barion, G. Bedeschi, V. Benesova, S. Bertelli, V. Bertone, C. Bissolotti, M. Boglione, G. Bozzi, *et al.*, arXiv preprint arXiv:2504.16034 (2025).

[41] S. Joosten and Z.-E. Meziani, arXiv preprint arXiv:1802.02616 (2018).

[42] E. Perez and E. Rizvi, Reports on Progress in Physics **76**, 046201 (2013).

[43] The NNPDF Collaboration, Nature **608**, 483 (2022).